Title
STAGNATION-POINT COMBUSTION WITH RADIATION

Authors
Kinoshita, CM.
Pagni, P.J.

Publication Date
1981-05-01

LBL-12769

Lawrence Berkeley Laboratory

UNIVERSITY OF CALIFORNIA

ENERGY & ENVIRONMENT DIVISION

Presented at the Eighteenth International Symposium on Combustion, University of Waterloo, Waterloo, Ontario, Canada, August 17-22, 1980; and to be published in the Proceedings

STAGNATION-POINT COMBUSTION WITH RADIATION

C.M. Kinoshita and P.J. Pagni

May 1981

Prepared for the U.S. Department of Energy under Contract W-7405-ENG-48

LBL-12769

STAGNATION-POINT COMBUSTION WITH RADIATION

C. M. Kinoshita and P. J. Pagni

May 1981

Mechanical Engineering Department

and

Lawrence Berkeley Laboratory
University of California
Berkeley, CA 94720

This work was supported by the Center for Fire Research of the U.S.D.O.C. National Bureau of Standards under Grant No. NB 80 NAG-E6839 which was administered by the U.S. Department of Energy under Contract No. W-7405-ENG-48.

STAGNATION-POINT COMBUSTION WITH RADIATION

C. M. Kinoshita and P. J. Pagni

Mechanical Engineering Department
and
Lawrence Berkeley Laboratory
University of California
Berkeley, California 94720 USA

Abstract

The relatively simple character of diffusion flames in laminar stagnation-point flows has led to numerous theoretical and experimental studies of that system. Here, as a first step toward incorporating radiation in analyses eventually related to fire safety, a grey radiating diffusion flame above a grey pyrolyzing solid fuel is considered. Shvab-Zeldovich variables are used in the analyses of steady, laminar, radiative, axisymmetric and Cartesian two-dimensional stagnation-point boundary layers. The velocity, temperature, and species fields are similar to analogous free convection flames. Two radiation approximations are compared for the case of a uniform absorption coefficient: (1) the exponential kernel and (2) the optically thin limit. The difference between these approximations proved insignificant; the simpler optically thin limit may be the method of choice. The results depend on eight parameters - five from non-radiating combustion: r, the mass consumption number; B, the mass transfer number; D_c, a dimensionless heat of combustion; θ_w, the fuel surface temperature; and Pr, the Prandtl number; and three radiation parameters: N_1 - a conduction/gaseous-radiation parameter; N_2 - a conduction/ambient-radiation parameter and ε, the surface emissivity. For conditions typical of synthetic polymer fuels, surface emission dominates gaseous radiation to the fuel and the pyrolysis rate is slightly lower than a non-radiative analysis would predict. Excess pyrolyzate calculations for radiating systems are included.

Introduction

The relatively simple, quasi-one-dimensional nature of diffusion flames in lamanar stagnation-point flows has encouraged analyses [1-9] of that system. Motivated by the importance of flame radiation to fire safety [10], the present study extends previous work [8,11] to the opposed flow diffusion flame apparatus, where proper determination of material properties from experimental data requires quantification of the net radiative effect on heat transfer at the pyrolyzing surface.

In this combustion system a stream of oxidizer approaches the stagnation point on a condensed fuel surface and reacts with pyrolyzed fuel in a thin diffusion flame within a constant thickness boundary layer. The fuel surface is assumed gray and diffuse and the gas is considered spectrally gray. Only the pyrolysis region is considered.

Analyses

The present mathematical formulation builds on previous non-radiative analyses [7,9] and hence is slightly abbreviated. Let x and y denote orthogonal spatial coordinates tangential and normal to the fuel surface respectively. The continuity, momentum, species and energy equations are, in turn,

$$\frac{\partial}{\partial x}(\rho u x^{\kappa}) + \frac{\partial}{\partial y}(\rho v x^{\kappa}) = 0 \tag{1a}$$

$$\rho u \frac{\partial u}{\partial x} + \rho v \frac{\partial u}{\partial y} = \frac{\partial}{\partial y}\left(\mu \frac{\partial u}{\partial y}\right) + \rho_\infty u_\infty \frac{du_\infty}{dx} \tag{1b}$$

$$\rho u \frac{\partial Y_i}{\partial x} + \rho v \frac{\partial Y_i}{\partial y} = \frac{\partial}{\partial y}\left(\rho D \frac{\partial Y_i}{\partial y}\right) + \dot{m}_i''' \tag{1c}$$

$$\rho u \frac{\partial h}{\partial x} + \rho v \frac{\partial h}{\partial y} = \frac{\partial}{\partial y}\left(\frac{\lambda}{c_p} \frac{\partial h}{\partial y}\right) - \frac{\partial \dot{q}_r''}{\partial y} + \dot{q}''' \tag{1d}$$

in which $\kappa=0$ for cartesian flow and $\kappa=1$ for axisymmetric flow, $\dot{q}_r''$ denotes the radiant heat flux and triple prime indicates per unit volume.

A fast single-step, overall chemical reaction is assumed and Shvab-Zeldovich coupling functions (β_1 and β_2) are employed to eliminate the generation terms in the species and energy governing equations. These coupling functions are normalized to form J_j and the following coupled species and energy-species equations for unit Lewis number are obtained:

$$\rho u \frac{\partial J_1}{\partial x} + \rho v \frac{\partial J_1}{\partial y} = \frac{\partial}{\partial y} (\rho D \frac{\partial J_1}{\partial y}) \tag{2a}$$

and

$$\rho u \frac{\partial J_2}{\partial x} + \rho v \frac{\partial J_2}{\partial y} = \frac{\partial}{\partial y} (\rho D \frac{\partial J_2}{\partial y}) + \frac{1}{(\frac{QY_{o\infty}}{\nu_o W_o} - h_w)} \frac{\partial \dot{q}_r''}{\partial y} \quad . \tag{2b}$$

The same similarity variables [9], $\eta \equiv (u_\infty/\nu_\infty x)^{\frac{1}{2}} \int_o^y \rho/\rho_\infty dy$ and $f(\eta) \equiv \psi(u_\infty \nu_\infty x)^{-\frac{1}{2}} x^{-\kappa}$ used in non-radiating, stagnation-point flow combustion are again employed. Assuming constant Pr, ρD and $\rho\mu$, the transformed momentum, species and energy-species equations become, respectively,

$$f''' + (\kappa+1)ff'' - (f')^2 + \theta = 0 \tag{3a}$$

$$J_1'' + (\kappa+1)\text{Pr}fJ_1' = 0 \tag{3b}$$

$$J_2'' + (\kappa+1)\text{Pr}fJ_2' = R \tag{3c}$$

in which primes denote differentiation with respect to η, and

$$R \equiv - \frac{\text{Pr}}{\{A/(\kappa+1)\}\rho(\frac{QY_{o\infty}}{\nu_o W_o} - h_w)} \frac{\partial \dot{q}_r''}{\partial y} \tag{4}$$

is a dimensionless radiant heat flux gradient. Assuming uniform molecular weight across the boundary layer in an ideal gas equation of state, $\theta \equiv T/T_\infty = \rho_\infty/\rho$. For non-radiating flows, R=0 and $J_1=J_2$. The boundary conditions for the transformed equations are [9]

$$f'(0) = 0 \quad , \quad J_1(0) = J_2(0) = 1 \quad , \tag{5a}$$

$$f'(\infty) = 1 \quad , \quad J_1(\infty) = J_2(\infty) = 0 \quad , \tag{5b}$$

while the remaining boundary condition on f will come, as usual, from a surface energy balance.

Species and temperature fields are obtained by imposing the flame-sheet approximation:

$$\begin{aligned} Y_f/Y_{fwo} &= r(J_1/J_{1f\ell}-1) \quad , \quad Y_o/Y_{o\infty} = 0 \quad , \\ \theta &= (\theta_w-1)[D_c-(D_c-1)J_2] + 1 \quad , \quad \eta < \eta_{f\ell} \quad , \end{aligned} \tag{6a}$$

while

$$\begin{aligned} Y_f/Y_{fwo} &= 0 \quad , \quad Y_o/Y_{o\infty} = 1-J_1/J_{1f\ell} \quad , \\ \theta &= (\theta_w-1)[D_c J_1/J_{1f\ell} - (D_c-1)J_2] + 1 \quad , \quad \eta > \eta_{f\ell} \quad , \end{aligned} \tag{6b}$$

in which constant c_p is assumed in the temperature expressions.

The fuel and energy balances at the pyrolyzing surface again yield the dimensionless pyrolysis rate, $-f(0)$, and the mass fraction of fuel at the surface,

$$\begin{aligned} -f(0) &= \frac{\rho_w v_w}{(\kappa+1)\rho_\infty(\{A/(\kappa+1)\}\nu_\infty)^{\frac{1}{2}}} \\ &= \frac{B}{(\kappa+1)\mathrm{Pr}}\left[-J_2'(0) - \left(\frac{\nu_\infty}{\{A/(\kappa+1)\}}\right)^{\frac{1}{2}} \frac{1}{(D_c-1)(\theta_w-1)} \frac{\dot{q}_{rw}''}{\lambda_\infty T_\infty}\right] , \end{aligned} \tag{7}$$

and

$$\frac{Y_{fw}}{Y_{fwo}} = \frac{Y_{ft}}{Y_{fwo}} - \left(\frac{r + Y_{ft}/Y_{fwo}}{1 + [(\kappa+1)\mathrm{Pr}f(0)/J_1'(0)]}\right) . \tag{8}$$

With this f(0), the pyrolysis rate, $\dot{M}_p$, and unburned fraction of total pyrolyzate, $\dot{M}_e/(Y_{ft}\dot{M}_p)$, are found directly from the respective non-radiative equations (14 and 15) of Ref. 9.

Radiation Approximations

For an absorbing-emitting, non-scattering medium adjacent to a gray diffuse surface, the radiant heat flux and incident energy per unit area are, respectively [12],

$$\dot{q}_r''(\tau) = 2b_w E_3(\tau) + 2\int_0^\tau \sigma T^4(t) E_2(\tau-t)dt - 2\int_\tau^\infty \sigma T^4(t) E_2(t-\tau)dt \tag{9a}$$

and

$$\dot{g}''(\tau) = 2b_w E_2(\tau) + 2\int_0^\infty \sigma T^4(t) E_1(|\tau-t|)dt \tag{9b}$$

where b_w denotes the fuel surface radiosity, τ is the local optical depth of the gas given by

$$\tau \equiv \int_0^y a dy \quad , \tag{10}$$

in which a is the absorption coefficient of the gas, and $E_k(\tau)$ is the kth exponential integral.

It is clear that evaluation of the exponential integrals in the dimensionless heat flux gradient, R, and the pyrolysis rate, -f(0), demands excessive computation. Instead, two approximations are used: (1) the exponential kernel approximation, see Appendix A, and (2) the optically thin limit.

Optically Thin Approximation

This limit results in considerable simplification of heat transfer calculations since only a single integral appears in the analysis as a boundary condition and the local heat flux gradient depends only on the local temperature rather than an integral of the temperature field. The thin approximation produces accurate results for film optical depths < 0.1, which is typical for laminar combustion of solid polymer fuels. Expansion of the exponential integrals [12] yields for $\tau \ll 1$,

$$E_2(\tau) \approx 1 \quad \text{and} \quad E_3(\tau) \approx \frac{1}{2} - \tau \tag{11}$$

The radiant heat flux, from Eq (9a), is then

$$\dot{q}_r''(\tau) \approx b_w(1-2\tau) - \sigma T_\infty^4(1-2\tau_\infty+2\tau) + 2\int_0^\tau \sigma T^4(t)dt - 2\int_\tau^{\tau_\infty} \sigma T^4(t)dt \tag{12}$$

and

$$\frac{d\dot{q}_r''}{d\tau} \approx -2(b_w+\sigma T_\infty^4) + 4\sigma T^4 \tag{13}$$

It is assumed that $T \simeq T_\infty$ for $\tau \geq \tau_\infty$. The dimensionless radiant heat flux gradient (see Eq.(3c)) is then from Eqs.(4, A7-A9, 12 and 13)

$$R = -\frac{N_1\theta}{N_2^2(D_c-1)(\theta_w-1)}\left[-2\{(\theta_w^4+1) - \left(\frac{1-\varepsilon}{\varepsilon}\right)\frac{\dot{q}_{rw}''}{\sigma T_\infty^4}\} + 4\theta^4\right] \tag{14}$$

where

$$\frac{\dot{q}_{rw}''}{\sigma T_\infty^4} = \varepsilon\left[(\theta_w^4-1) - \frac{2N_1}{N_2}\int_0^{\eta_\infty}(\theta^5-\theta)d\eta\right] , \tag{15}$$

The pyrolysis rate incorporating radiation, Eq.(7), now becomes

$$-f(0) = \frac{B}{(\kappa+1)Pr}\{-J_2'(0) - \frac{1}{N_2(D_c-1)(\theta_w-1)}\varepsilon\left[(\theta_w^4-1) - \frac{2N_1}{N_2}\int_0^{\eta_\infty}(\theta^5-\theta)d\eta\right]\} . \tag{16}$$

Results

The eight dimensionless parameters which control the system under investigation are five combustion groups - the mass transfer no., B, the mass consumption no., r, a dimensionless heat of combustion, D_c, the fuel surface temperature, θ_w, the Prandtl no., Pr and three radiation groups - a conduction/gaseous-radiation parameter, N_1, a conduction/ambient-radiation parameter, N_2, and the fuel surface emissivity, ε. Each parameter was varied over a typical range. Unless otherwise noted, the following values, representative of weakly radiating synthetic polymers, were used for most sample solutions presented here: $B=1.0$, $r=0.22$, $D_c=5.0$, $\theta_w=2.0$, $Pr=0.73$, $N_1=0.05$, $N_2=50.0$ and $\varepsilon=1.0$.

For the numerical solutions, Eqs. (3), and (A10 and A12) in the kernel substitution approximation or (14) in the optically thin approximation, were first linearized. All derivatives were then represented in standard three-point finite difference form. (This requires introducing f' as an additional variable since f''' cannot be represented in a three-point scheme.) As in all similar problems, the boundary conditions at infinity were imposed at some finite location, $\eta=\eta_\infty$. The difference equations were then recast in block tri-diagonal matrix form and solved employing an optimal pivoting strategy. Old values resulting from the quasi-linearization technique were then replaced by new values and the process repeated. This iterative cycle was terminated when all unknown values or gradients of variables at both boundaries had converged to within 10^{-5}. For the computations, 100 grid points were deployed across the boundary layer, $0\leq\eta\leq\eta_\infty$. $\eta_\infty=10$ was found to be sufficiently large for typical calculations. m=1 and n=2 were selected for the kernel approximation as these yield correct values of E_2 and E_3 at $\tau=0$.

Temperature, species, and velocity profiles for axisymmetric, non-radiating (N_1=0, N_2=∞) and radiating (N_1=0.1, N_2=10.0) systems obtained with both radiation approximations are presented in Fig. 1. Two-dimensional Cartesian combustion is analogous to axisymmetric combustion in every respect. Since the agreement between radiation models is excellent, hereafter, only the simpler, optically thin approximation is discussed. For this system, $\tau_\infty = N_1/N_2 \int_0^{\eta_\infty} \theta d\eta \lesssim 0.1$, hence the error in the optically thin approximation, of order τ_∞, is slight and the error in the combined conduction and radiation heat transfer rate even less.

Under the typical conditions imposed in Fig. 1, the surface emission exceeds the incoming radiation from the hot gas producing a net radiant heat flux out of the fuel surface. The overall heat transfer rate into the surface thus decreases with radiation and a lower pyrolysis rate is obtained which yields a shorter flame standoff distance and smaller surface fuel concentration. The flame temperature decreases with the inclusion of radiation since gaseous emission affords a parallel mechanism to conduction for heat loss from the reaction zone. As in a previous study [8] at fixed pryolysis rate, radiative effects produce a flatter temperature distribution. The pressure gradient in stagnation-point flow accelerates the lower density gas near the flame causing the velocity in the boundary layer to exceed the free-stream velocity. Since the flame temperature is lower with radiation, a weaker density variation results which produces less velocity overshoot.

Figure 2 plots the dimensionless pyrolysis rate, $-f(0)$, and net radiation from the surface, $\dot{q}_{rw}''/\sigma T_\infty^4$, versus conduction/radiation parameter, N_1, in both geometries. For the parameters specified, in spite of a substantial variation in wall radiation, the pyrolysis rate is nearly independent of N_1 over this small range. As N_1 increases, the flame radiation into the surface increases ($\dot{q}_{rw}''$ decreases) which increases slightly the pyrolysis rate. The variation in pyrolysis rate with N_1 is small, however, because the parallel conduction to the surface decreases as radiation increases due to both a decrease in flame temperature with increasing gaseous emission and an offsetting effect of blowing on conduction as pyrolysis increases. Additional calculations at other values of N_2 show the similar trends, i.e., a decrease in surface radiation efflux which produces only a slight increase in pyrolysis rate with increasing N_1. Effectively, N_1,influences the balance between conduction and radiation but not the total flux to the surface. The pyrolysis rate with radiation may be lower (here ~10%) than without radiation even for conditions in which irradiation from the hot gas and surface emission effectively cancel, because of the decrease in flame temperature which decreases conduction. More dramatic change in the pyrolysis rate may be ovserved for a higher, more realistic θ_w.

The same pair of dependent variables, $-f(0)$ and $\dot{q}_{rw}''/\sigma T_\infty^4$, are plotted against N_2 in Fig. 3. Both $\dot{q}_{rw}''/\sigma T_\infty^4$ and $-f(0)$ increase as N_2 increases as indicated by Eqs. (15 and 16) respectively. In the limit $N_2 \to \infty$, no flame radiation exists and both surface emission and conduction to the surface are a maximum. Since the optical depth of the boundary layer increases making gaseous radiation important as N_2 decreases, the flame temperature drops decreasing conduction and consequently $f(0)$. Equation (16) suggests that of the two conduction/radiation parameters N_1 and N_2, the latter dominates the total heat flux to the surface and hence the pyrolysis rate.

Pyrolysis rate and unburned fraction of total pyrolyzate are presented as functions of mass transfer number, B, in Fig. 4 and mass consumption number, r, in Fig. 5 for axisymmetric radiating and non-radiating combustion. Again, the Cartesian results are very similar. The radiating case is slightly below the non-radiating case because surface emission dominates gaseous emission. Pyrolysis increases substantially as B increases as expected. The pyrolysis rate decreases slightly as r increases, as a result of a decrease in flame temperature ($\theta_{f\ell} \sim D_c/r$) which decreases the total energy feedback to the surface. This decrease is slightly larger when a second feedback mechanism - radiation - is introduced. In the non-radiating case, the fuel fraction at the surface is known a priori from Eqs. (7 and 8) as an explicit function of B, $Y_{o\infty}$, Y_{ft} and s, $Y_{fwo} = (Y_{ft}B - Y_{o\infty}s)/(B+1)$, hence Y_{fwo} vanishes as B decreases to $Y_{o\infty}s/Y_{ft}$ and combustion ceases. With radiation, however, Y_{fw} depends on all eight parameters and must be calculated simultaneously with the other dependent variables. Radiation causes combustion to cease more readily, i.e., Y_{fw} vanishes at higher B, since for the parameters specified here, the total heat transfer rate to the surface decreases when radiation is added. The unburned fraction of total pyrolyzate tends to increase as r decreases and B increases. The radiating flow produces slightly less excess pyrolyzate than the non-radiating flow, i.e., the effect of radiation is to make the flow appear as a non-radiating flow at a higher r and lower B.

Figure 6 plots pyrolysis rate and unburned fraction of total pyrolyzate versus dimensionless heat of combustion, D_c, for axisymmetric combustion. The pyrolysis rate increases strongly with increasing D_c, primarily because of an increase in flame temperature ($\theta_{f\ell} \sim \theta_w D_c$). Like the mass fraction of fuel at the surface, the dimensionless flame temperature, $\theta_{f\ell}$, which in non-radiating flows can be determined a priori from measurable quantities, depends on all eight parameters in radiating flows and is not predetermined. Again, the pyrolysis rate is lower with radiation due to a net efflux of radiation at the surface. As noted previously [9], both pyrolysis rate and excess pyrolyzate are fairly weak functions of D_c in non-radiating systems since D_c enters the non-radiating mathematical analysis only through θ in the momentum equation (3a). However, both pyrolysis rate and excess pyrolyzate vary very strongly with D_c in radiating flows since with radiation, D_c also appears in the energy-species equation (3c) through R, Eq. (14), which becomes singular as $D_c \to 1$, forcing $f(0) \to 0$ at a $D_c \gtrsim 1$; see Eq. (16). The parameter D_c is effectively a heat of combustion divided by a surface enthalpy. At low D_c, the reaction releases little energy to counter surface emission losses giving low pyrolysis rates, whereas at large D_c, much energy is released which easily overcomes surface losses and yields large pyrolysis rates. Increasing the wall temperature, θ_w, in non-radiating flow causes a slight increase in pyrolysis rate due to an increase in flame temperature. However, the decrease of the pyrolysis rate for the radiating case beneath the non-radiating case increases as θ_w increases, due to more surface emission. This strong dependence on D_c and θ_w shows that the radiative analysis not only introduces new parameters but also alters the import of parameters which appear in the non-radiative analysis. The practical consequenses of the alteration may be even more significant than of the introduction, since in a given system the variation with fuel and flow conditions of D_c and θ_w may be greater than the variation of N_1, N_2 or ε.

Conclusions

Steady, laminar, diffusion-controlled combustion of an absorbing-emitting gas in two-dimensional, axisymmetric and Cartesian stagnation-point flows is analyzed. Eight parameters, the mass transfer number, B, the mass consumption number, r, the Prandtl number, Pr, a dimensionless heat of combustion, D_c, the fuel surface temperature, θ_w, two conduction/radiation parameters, N_1 and N_2, and the fuel surface emissivity, ε, are required to describe the combusting-radiating system. The parameters D_c and θ_w, which were of secondary importance in non-radiating systems, emerge from the radiative analysis with a new significance, dominating the newly introduced parameters, N_1, N_2 and ε. The flame temperature and mass fraction of fuel at the surface depend on all eight parameters and, unlike combustion without radiation, cannot be determined _a priori_. The difference between the radiation approximations considered, the exponential kernel and the optically thin limit, is insignificant for typical laminar burning conditions. In general, the influx of gaseous radiation is insufficient to cancel the efflux of surface emission, hence a lower pyrolysis rate, in comparison to non-radiative combustion, results. Lower pyrolysis rates may result even when a net influx of radiation prevails because of the decrease in conduction caused by the lower flame temperature due to radiant loss from the combustion zone.

The net effect of radiation on pyrolysis seems small for several reasons. The properties of real opposed flow diffusion flames are not yet sufficiently well known to give accurate parameter values. Those chosen here, $\theta_w = 2$, $N_1 = 0.05$ (perhaps too small) and $D_c = 5$, $N_2 = 50$ (perhpas too large) all tend to underestimate the differences between non-radiating and radiating systems. Results for a second set ($\theta_w = 3$, $N_1 = 1$, $D_c = 3$ and $N_2 = 10$), together with the results presented,would properly bracket synthetic polymer fueled systems. In addition, there exist physical interactions which tend to mitigate radiation effects in this small scale system. Surface emission is somewhat cancelled by flame radiation. Conduction is reduced due to lowered flame temperatures when radiation is introduced as a parallel path for heat transfer from the flame to the surface. Conduction is also reduced by blowing whenever the pyrolysis rate is increased due to a net increase in heat transfer to the surface.

In the future as data on optical properties of stagnation-point flames become available, the approximation of a constant absorption coefficient should be replaced with a non-uniform a based on measured distributions of soot volume fractions and CO_2 and H_2O concentrations. Some utility for this analysis will then come both from proper quantification of radiative effects on material property measurements in opposed flow diffusion flame apparati and from the use of such systems to refine techniques for incorporating radiation in combustion modeling.

ACKNOWLEDGEMENT

This work was supported by the Center for Fire Research of the U.S.D.O.C., National Bureau of Standards under Grant No. NB 80 NAG-E6839 which was administered by the U.S. Department of Energy under Contract No.W-7405-ENG-48.

NOMENCLATURE

A	constant in stagnation-point free-stream velocity ,$u_\infty(x,y)/x$ as $y \to 0$
a	absorption coefficient
B	mass transfer number, $(QY_{o\infty}/\nu_o W_o - h_w)/L$
b	radiosity
c_p	specific heat
D	species diffusivity
D_c	dimensionless heat of combustion, $QY_{o\infty}/\nu_o W_o h_w$
$\dot{g}''$	incident radiant energy flux
h	specific enthalpy, $\int_{T_\infty}^{T} c_p dT$
J_j	normalized Shvab-Zeldovich coupling variable, $(\beta_j - \beta_{j\infty})/(\beta_{jw} - \beta_{j\infty})$
L	effective latent heat of pyrolysis
N_1	$\lambda_\infty a/T_\infty^{\ 3}$
N_2	$\dfrac{\lambda_\infty}{\sigma T_\infty^{\ 3}} \left(\dfrac{A}{(\kappa+1)\nu_\infty}\right)^{1/2}$
Q	energy released by combustion of ν_f moles of gas phase fuel
R	dimensionless radiation heat flux gradient
r	mass consumption number, $Y_{o\infty}s/Y_{fwo}$

s stoichiometric ratio, $\nu_f W_f/\nu_o W_o$

W_i molecular weight of species i

Y_i mass fraction of species i

Y_{fw} wall fuel mass fraction

Y_{fwo} wall fuel mass fraction without radiation, $(Y_{ft}B-Y_{o\infty}s)/(1+B)$

Symbols

β_1 Shvab-Zeldovich species coupling variable, $Y_f/\nu_f W_f - Y_o/\nu_o W_o$

β_2 Shvab-Zeldovich energy-species coupling variable, $-h/Q-Y_o/\nu_o W_o$

ε surface emissivity

θ dimensionless temperature, T/T_∞

λ conductivity

ν kinematic viscosity or stoichiometric coefficient

σ Stefan-Boltzmann constant

τ optical depth

Subscripts

f fuel

$f\ell$ flame

o oxidizer

t transferred gas

w fuel surface

∞ ambient

Appendix A

Exponential Kernel Substitution

The exponential integral, $E_k(\tau)$, may be approximated with the following exponential form:

$$E_2(\tau) = me^{-n\tau} \quad . \tag{A1}$$

Then from Eqs. (9)

$$\dot{q}_r''(\tau) = \frac{2b_w me^{-n\tau}}{n} + 2\int_0^\tau \sigma T^4(t) me^{-n(\tau-t)}dt - 2\int_\tau^\infty \sigma T^4(t) me^{-n(t-\tau)}dt \tag{A2}$$

and

$$\dot{g}''(\tau) = 2b_w me^{-n\tau} + 2\int_0^\infty \sigma T^4(t) mne^{-n|\tau-t|}dt \quad . \tag{A3}$$

It can be verified by substitution that

$$\frac{d^2\dot{g}''}{d\tau^2} - n^2\dot{g}'' = -4mn^2\sigma T^4 \tag{A4a}$$

and

$$\frac{d\dot{q}_r''}{d\tau} = -\dot{g}'' + 4m\sigma T^4 \quad . \tag{A4b}$$

Also,

$$\dot{g}'' - \frac{1}{n}\frac{d\dot{g}''}{d\tau} = 4mb_w \quad \text{at} \quad \tau = 0 \quad , \tag{A5}$$

$$\dot{g}'' + \frac{1}{n}\frac{d\dot{g}''}{d\tau} = 4m\sigma T_\infty^{\ 4} \quad \text{at} \quad \tau = \tau_\infty \quad , \tag{A6}$$

where it is assumed that $T \approx T_\infty$ for $\tau \geq \tau_\infty$, with τ_∞ yet to be determined.

For the gray diffuse fuel surface the radiosity is [12],

$$b_w = \sigma T_w^{\ 4} - \left(\frac{1-\varepsilon}{\varepsilon}\right) \dot{q}_{rw}'' \tag{A7}$$

in which ε is the emissivity of the fuel surface. Since

$$d\tau = a\,dy = \frac{N_1}{N_2}\,\theta\,d\eta \quad , \tag{A8}$$

where

$$N_1 \equiv \frac{\lambda_\infty a}{\sigma T_\infty^{\;3}} \quad , \quad N_2 \equiv \frac{\lambda_\infty}{\sigma T_\infty^{\;3}} \left(\frac{\{\Lambda/(\kappa+1)\}}{\nu_\infty}\right)^{\frac{1}{2}} \quad . \tag{A9}$$

Equations (A5–A9) yield, for constant absorption coefficient

$$\left(\frac{N_2}{N_1}\right)^2 \frac{1}{\theta}\left(\frac{G'}{\theta}\right)' - n^2 G + 4mn^2\theta^4 = 0 \quad , \tag{A10}$$

subject to the conditions

$$G(0) - \frac{N_2}{N_1 n^2 \theta_w}\left[n + 4m\left(\frac{1-\varepsilon}{\varepsilon}\right)\right] G'(0) = 4m\theta_w^{\;4} \quad , \tag{A11a}$$

$$G(\eta_\infty) + \frac{N_2}{N_1 n} G'(\eta_\infty) = 4m \quad , \tag{A11b}$$

where $G \equiv \dot{g}''/\sigma T_\infty^{\;4}$. From Eqs. (4, A4 and A8),

$$R = -\frac{N_1\theta}{N_2^{\;2}(D_c-1)(\theta_w-1)}\left(-G + 4m\theta^4\right) \tag{A12}$$

while the dimensionless pyrolysis rate is found from Eqs. (7, A5, A7 and A9) with $\dot{q}_r'' = n^{-2}\, d\dot{g}''/d\tau$ to be

$$-f(0) = \frac{B}{(\kappa+1)\mathrm{Pr}}\left\{-J_2'(0) - \frac{1}{N_2(D_c-1)(\theta_w-1)}\left[-\frac{G(0) + 4m\theta_w^{\;4}}{n+4m\left(\frac{1-\varepsilon}{\varepsilon}\right)}\right]\right\} . \tag{A13}$$

ACKNOWLEDGEMENTS

This work was supported by the Center for Fire Research in the U.S.D.O.C. National Bureau of Standards under Grant No. NB 80 NAG-E6839 which was administered by the U.S. Department of Energy under Contract No. W-7405-ENG-48.

REFERENCES

1. Seshadri, K., and Williams, F. A., *J. Polymer Science: Polymer Chemistry Ed.*, *16*, 1755-1778 (1978).

2. Tsuji, H., and Yamaoka, I., *Twelfth Symposium (Int'l) on Combustion*, 997-1005, The Combustion Institute (1969).

3. Tsuji, H., and Yamoka, I., *Thirteenth Symposium (Int'l) on Combustion*, 723-731, The Combustion Institute (1971).

4. Pitz, W. J., Brown, N. J., and Sawyer, R. F., "The Structure of a Poly(ethylene) Opposed Flow Diffusion Flame," This Symposium.

5. Holve, D. J., and Sawyer, R. F., *Fifteenth Symposium (Int'l) on Combustion*, 351-361, The Combustion Institute (1975).

6. Matthews, R. D., and Sawyer, R. F., *J. Fire and Flamm.*, 7, 200-216 (1976).

7. Krishnamurthy, L., and Williams, F. A., *Acta Astronautica*, *1*, 711-736 (1974).

8. Negrelli, D. E., Lloyd, J. R., and Novotny, J. L., *ASME J. Heat Transfer*, *99*, 212-220 (1977).

9. Kinoshita, C. M., Pagni, P. J., and Beier, R. A., "Opposed Flow Diffusion Flame Extensions," This Symposium.

10. de Ris, J., *Seventeenth Symposium (Int'l) on Combustion*, 1003-1016, The Combustion Institute (1978).

11. Kinoshita, C. M., "Stagnant-Film Combustion of an Absorbing-Emitting Gas," to be published in *Combustion and Flame*.

12. Sparrow, E. M., and Cess, R. D., *Radiation Heat Transfer*, McGraw-Hill (1978).

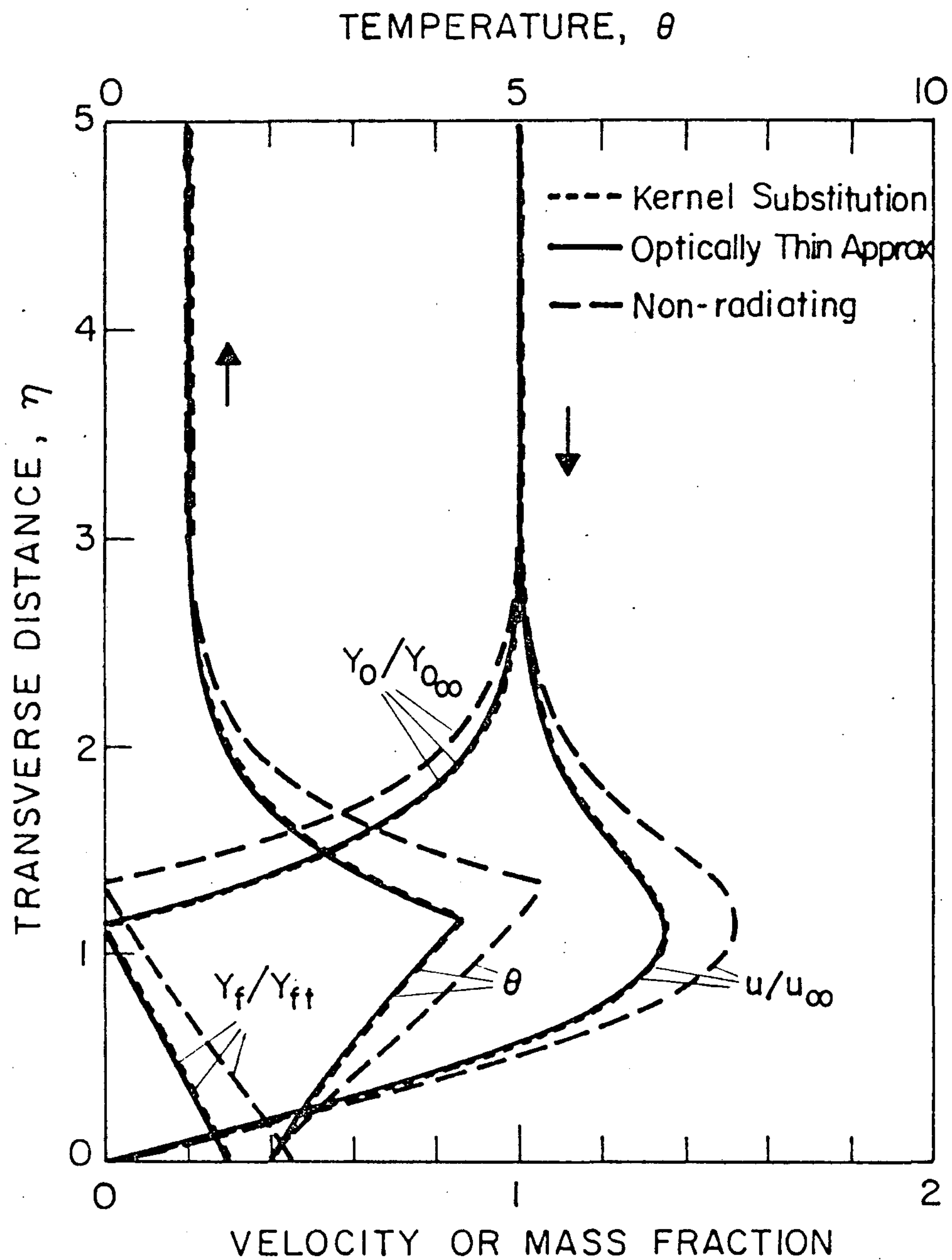

Fig. 1 Comparison of radiation models: Temperature, species, and velocity profiles for axisymmetric, opposed flow diffusion flames with $B = 1.0$, $r = 0.22$, $D_c = 5.0$, $\theta_w = 2.0$, $N_1 = 0.1$, $N_2 = 10.0$, and $\varepsilon = 1.0$.

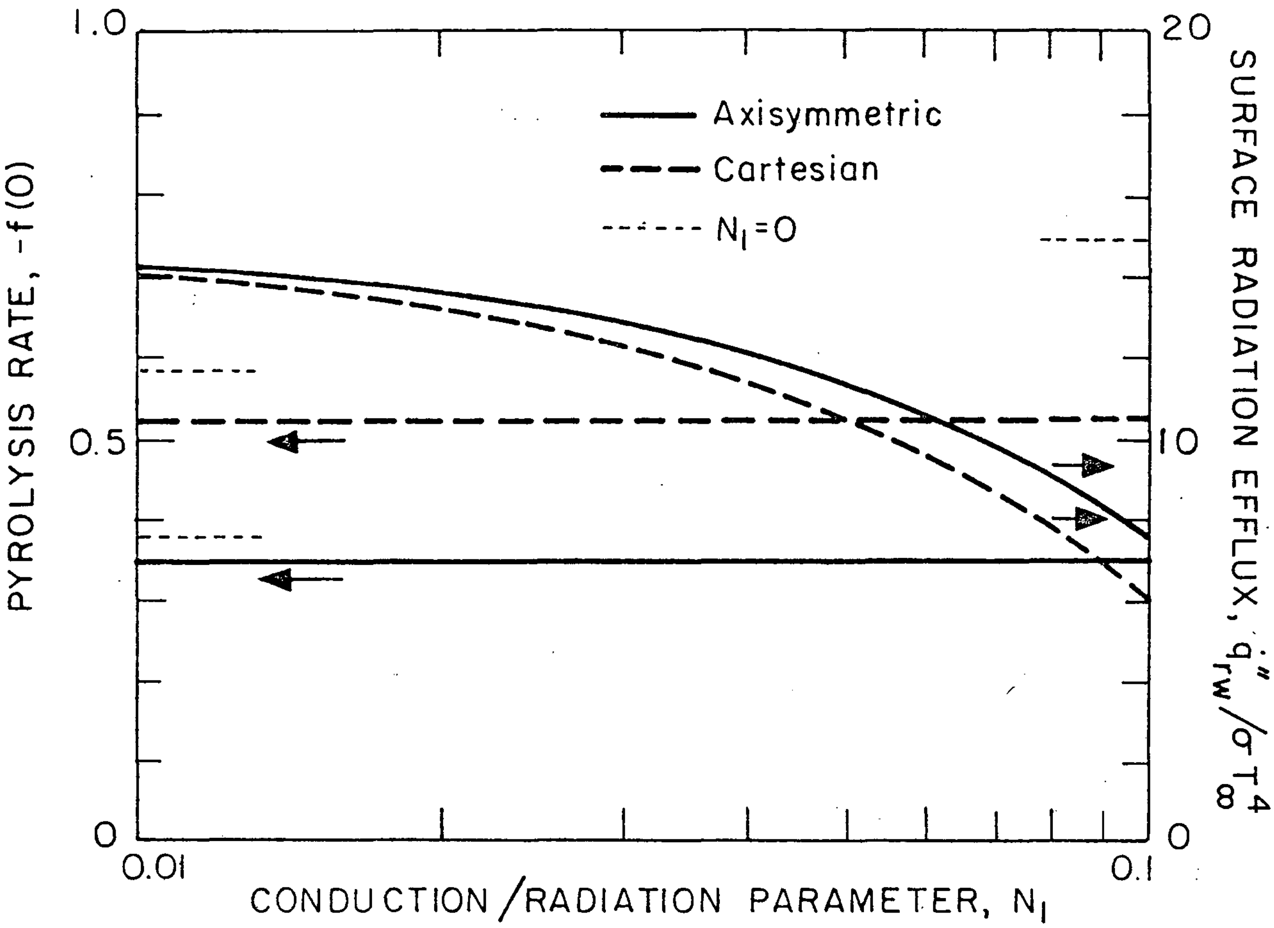

Fig. 2 Pyrolysis rate and surface radiation efflux versus $N_1 = \lambda_\infty a/\sigma T_\infty^3$, a conduction/gaseous-radiation parameter, for $B = 1.0$, $r = 0.22$, $D_c = 5.0$, $\theta_w = 2.0$, $N_2 = 50.0$, and $\varepsilon = 1.0$.

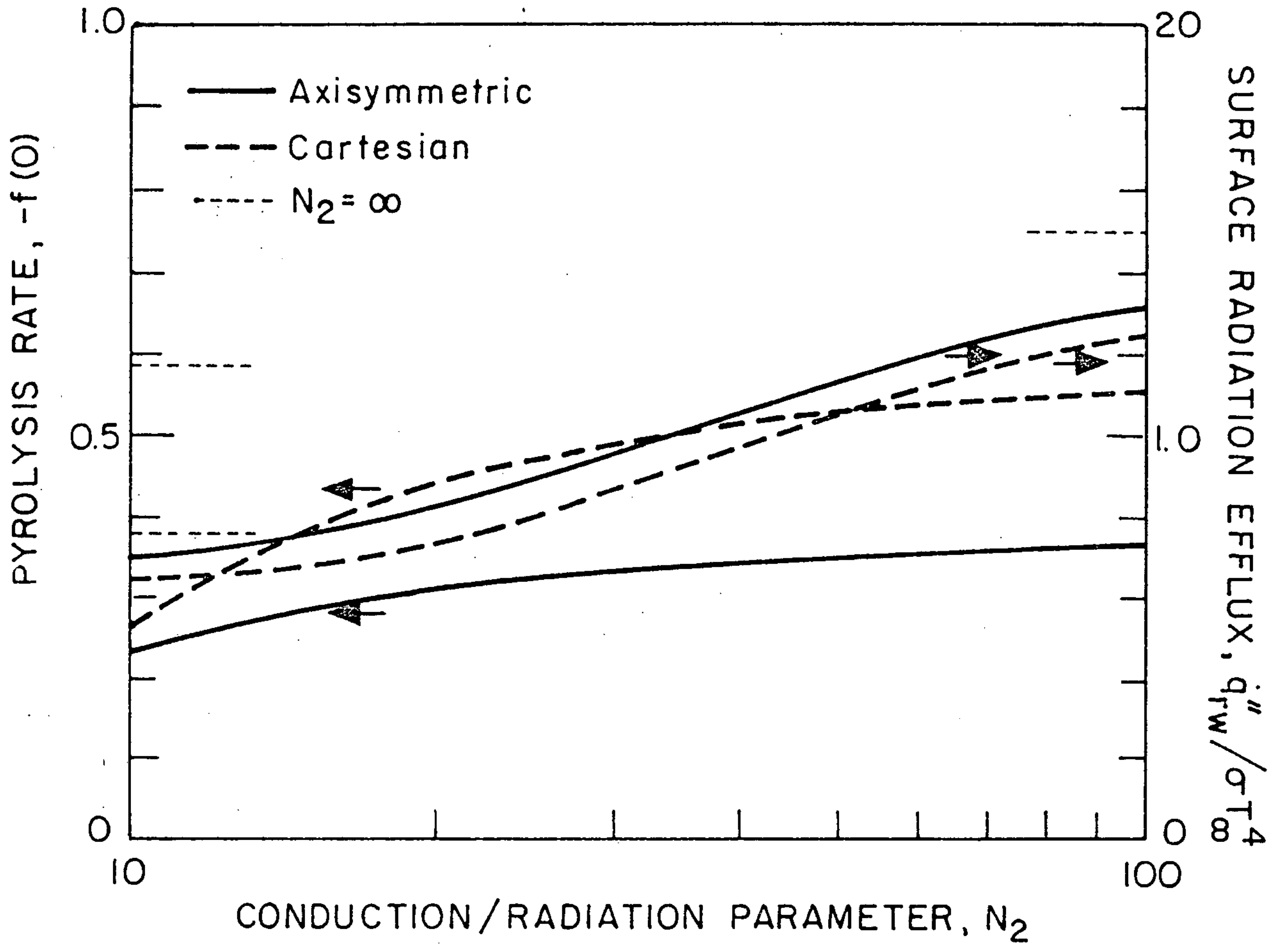

Fig. 3 Pyrolysis rate and surface radiation efflux versus $N_2 = \frac{\lambda_\infty}{\sigma T_\infty^3} \left(\frac{A}{(\kappa+1)\nu_\infty}\right)^{\frac{1}{2}}$, a conduction/ambient-radiation parameter, for $B = 1.0$, $r = 0.22$, $D_c = 5.0$, $\theta_w = 2.0$, $N_1 = 0.05$, and $\varepsilon = 1.0$.

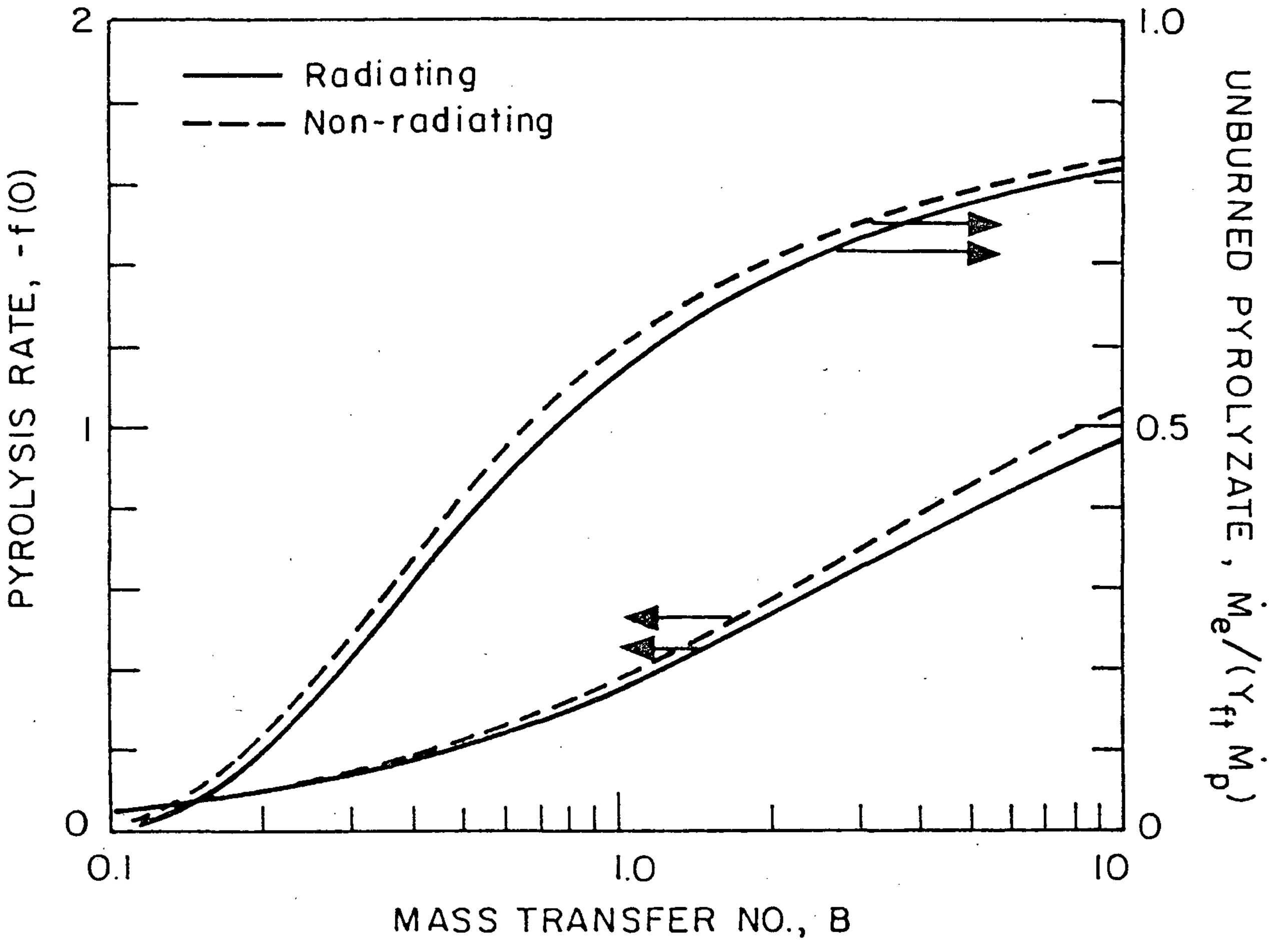

Fig. 4

Pyrolysis rate and unburned pyrolyzate versus mass transfer number for axisymmetric flow with $D_c = 5.0$, $\theta_w = 2.0$, $N_1 = 0.05$, $N_2 = 50.0$, $\varepsilon = 1.0$, and $r = (B+1)/(10B-1)$.

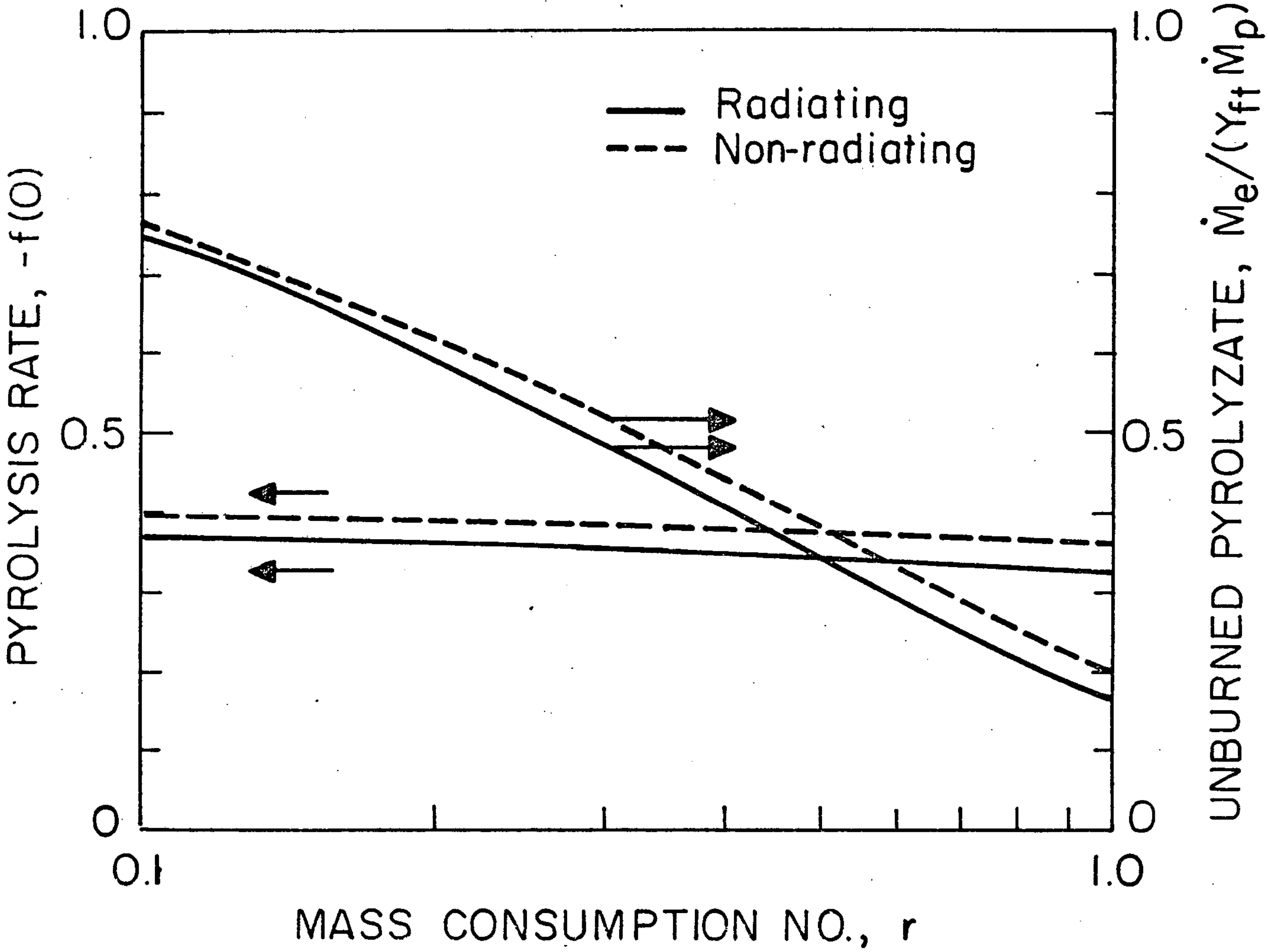

Fig. 5 Pyrolysis rate and unburned pyrolyzate versus mass consumption number for axisymmetric flow with $B = 1.0$, $D_c = 5.0$, $\theta_w = 2.0$, $N_1 = 0.05$, $N_2 = 50.0$, and $\varepsilon = 1.0$.

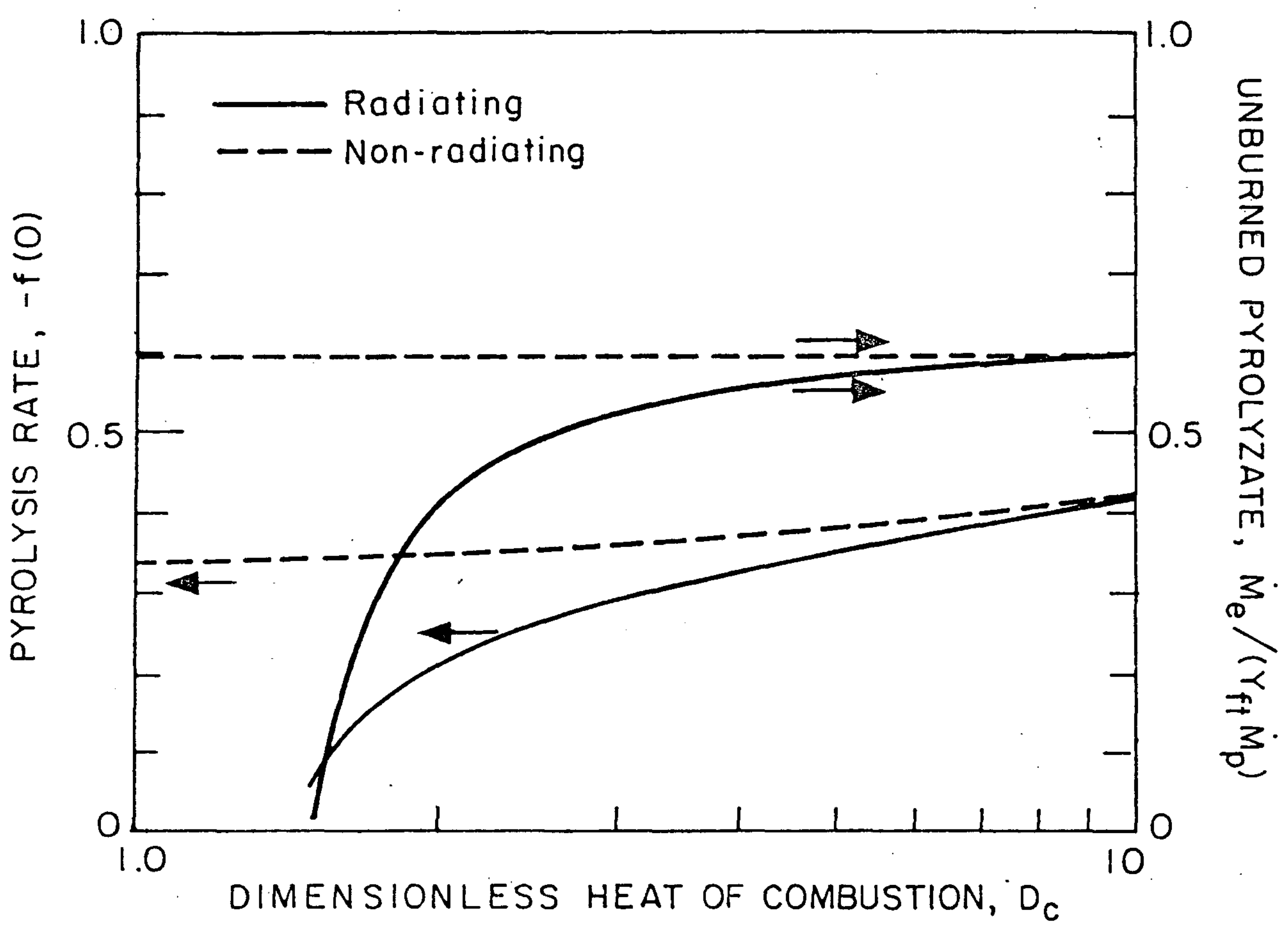

Fig. 6 Pyrolysis rate and unburned pyrolyzate versus dimensionless heat of combustion for axisymmetric flow with $B = 1.0$, $r = 0.22$, $\theta_w = 2.0$, $N_1 = 0.05$, $N_2 = 50.0$, and $\varepsilon = 1.0$.